The Effect of alpha-Synuclein Aggregates on Astrocyte Calcium Signaling in Neurodegeneration

University of
St Andrews

ELENA RICO HERNANDO

Contact: erh21@st-andrews.ac.uk
Supervisors: Dr Vanya Metodieva and Dr Juan Varela
August 2023

Introduction:

Parkinson's disease (PD) affects between 1-2% of the population aged over 65, being the second most common neurodegenerative disease after Alzheimer's disease.[1] The neuropathological indication of the disease is the presence of Lewy bodies in the *substancia nigra pars compact*a, which are composed of the proteins αSynuclein, ubiquitin and many others.[2,3]

Synucleins are proteins found to be abundant in the brain consisting of three members: αSynuclein, βSynuclein and γSynuclein.[4,5] αSynuclein is a 140 amino acid protein with an α-helix structure found in neurons and Lewy bodies.[6] Abnormal aggregation of this protein is a crucial pathological feature of neurogenerative diseases called synucleinopathies.[7] These abnormal forms of αSynuclein trigger neuronal death through mitochondrial impairment, lysosomal dysfunction and the changing of calcium homeostasis.[8] αSynuclein aggregation is one of the most prominent indicators of PD that is postulated to appear in the early onset of the disease and spread across the nervous system in the later stages.[9]

αSynuclein is an unfolded protein that can self-assemble into highly ordered aggregates (amyloid fibrils) upon incubation for longer time periods *in vitro*.[10] During this aggregation process from oligomers to fibrils, aggregates change from a random-coil confirmation to β-pleated sheets that have characteristics of amyloid fibrils as more species bind together. [11,12] αSynuclein monomer and oligomers (protofibrils) are soluble whereas fibrils are insoluble in neuronal cytoplasm which have different implications during disease.[13] This conformational change is vital as studies have shown that a structural conversion during αSynuclein makes oligomers more toxic[14] leading to neuronal death,[15,16,17] whereas fibrillar aggregates could have a protective mechanism in PD.[18,19] αSynuclein not only affects neurons but also glia. Spreading of excessive αSynuclein from neuronal cells has been outline as a possible mechanism of αSynuclein aggregation that causes the activation of inflammatory responses in glia and detrimental effects in synucleinopathies.[20]

Glial cells are the most abundant type of cells in the central nervous system (CNS).[21] It is known that these cells play a crucial role in supporting brain development and function.[22] Astrocytes are a type of glial cell characterized by a complex morphology that have extensive network formation with other astrocytes and a specialized contact with other structures such as synapses and the brain blood barrier.[23,24,25] A key feature of astrocytes are their ion channels and carriers that help to control and stabilize the environment for neurons to function,[26,27] and provide an electrolyte homeostasis.[28,29] In PD, astrocytes selectively adhere to dopaminergic neurons leading to a significant loss of these fibers and progressive degeneration of dopaminergic neurons that leads to a more rapid onset of PD.[30]

Astrocytes not only respond to intracellular stimuli but also to intercellular stimuli through the propagation of intercellular calcium waves (ICW) to adjacent non-stimulated astrocytes that is vital for CNS functioning.[31,32] ICW are defined as a localized increase of calcium ions that is followed by a wave-like succession of calcium events.[33] The propagation mechanism of calcium waves is still unknown.[34] Distinct calcium ion signals control blood vessel diameter, regulate gene expression, contribute to neuromodulation, and modulate potassium ion uptake amongst many other functions.[35, 36, 37,38]

PD and αSynuclein aggregation affect astrocytes through multiple mechanisms such as though inflammatory response or neuron degeneration. However, it is still unknown how αSynuclein affects astrocytic network communications and ICW, which have essential regulatory roles in the brain. This project aims to provide an insight into this by utilizing αSynuclein at different aggregation stages to find out how they affect astrocytic calcium waves using calcium imaging in brain slices. Finding out how ICW are affected by αSynuclein aggregates could provide information to design new therapeutic targets.

Methodology:

1. Murine organotypic hippocampal slices expressing GCaMP3

The murine organotypic hippocampal brain slices (OHBS) expressing the optogenetic construct were prepared by Dr Vanya Metodieva. Briefly, the brain slices were obtained from day 7 C57BL6 mice that were humanely sacrificed. The hippocampi were isolated and sliced into 350μm transverse slices. The slices were then plated on sterile culture inserts in sterile 6-well plates and supplied with fresh culture medium every 4 days. The OHBSs were kept in an incubator maintained at 34°C, 5% CO_2, humidified atmosphere. They were transduced by Dr Vanya Metodieva using AAV particles containing gfaABC1D-Cyto-GCaMP3 which was a gift from Baljit Khakh.

2. Synuclein aggregation

Lyophilized human recombinant αSynuclein monomers were reconstructed in 10mM sodium phosphate buffer (pH 7.4) The reconstruction was filtered using a 0.1μm filter on ice. After the reconstruction αSynuclein had a concentration of 70μM. The aggregates were then stored in a freezer at −80°C.

Prior to an aggregation reaction, αSynuclein monomeric stocks were defrosted on ice and placed in an orbital shaker incubator at 37°C, 200RPM. Aggregate samples were collected at 3h, 6h, 24h and 96h after the start of the aggregation.

3. Coverslip cleaning

Glass coverslips were cleaned by bath sonication in 100% isopropanol, 100% ethanol and deionized water, 10 minutes each step. The coverslips were then dried at 150°C for 15 minutes.

The coverslips were then plasma cleaned with an argon plasma generator for 1h. The slide chambers were then placed on each coverslip. They were then coated with filtered Poly-L-lysine (PLL) for 0.5h at RTP and washed 3 times with filtered phosphate buffered saline (PBS).

4. Aggregate imaging

Thioflavin T (ThT) was diluted in PBS, passed through a 0.1μm filter and stored at 4°C, protected from light. The concentration was calculated using the Beer–Lambert law:

$$C = \frac{A}{\varepsilon l}$$

ThT absorbance was measured using a plate reader and used at a final concentration of 5μM. Nile red was diluted to a final concentration of 2nM. αSynuclein was diluted to a final concentration of 1μM. The mix was applied on the coverslip for imaging.

Total internal reflection fluorescence (TIRF) (Nikon ECLIPSE Ti2 inverted) was used to characterize αSynuclein aggregates, NR and ThT images were acquired. The imaging conditions for NR were: 532nm laser illumination, 30mW power, 5000 frames and 50ms exposure time. ThT images were acquired using 405nm laser illumination, 10mW power, 50 frames and 50ms exposure time.

Image J was used for image analysis. All brightness and contrast levels were kept the same for ThT acquisitions. ThunderSTORM was used for the reconstruction of NR images.

5. Live imaging of calcium waves

The aggregates were thawed on ice and diluted to a final concentration of 1μM in growth medium. PBS was diluted in growth medium as a vehicle control. Slices were kept in artificial

cerebrospinal fluid (αCSF; NaCl 125mM, KCL 2.5mM, $MgCl_2$ 1mM, $CaCl_2$ 3mM, HEPES 10mM and Glucose 3.6mM) for the duration of the imaging. They were stabilized on a sterile surface using an imaging harp (Harvard Instruments) and allowed to equilibrate at room temperature for 5 minutes prior to imaging.

OHBSs were imaged using spinning disc confocal microscope (Yokogawa Nikon ECLIPSE Ti2) GCaMP3 was excited using 488nm laser at 50% laser power. Calcium activity was recorded at 60x magnification, 40ms exposure time, 2x2 binning, 12-bit depth. The recordings were 1 minute long.

6. Analysis of calcium waves using AQUA

Astrocytic calcium activity was analyzed using the MATLAB-based platform AQuA (Astrocyte Quantification and Analysis).[39] The data was exported in CSV format and Graphpad Prism was then used for data visualization and statistical analysis.

Results:

1. αSynuclein aggregation

Monomeric αSynuclein was aggregated for a period of 96h to generate structurally diverse aggregates which would be used to study αSynuclein-mediated effects on astrocyte signaling. Thioflavin T (ThT) was used to stain amyloidogenic proteins. ThT binds to the beta sheets of proteins showing amyloidogenic proteins. To observe the aggregates, total internal reflection fluorescence (TIRF) microscopy was used to image only the protein on the coverslip and minimize background fluorescence.

As seen in Figure 1, there was a progressive aggregation of monomers into oligomeric and fibrillar structures with time.

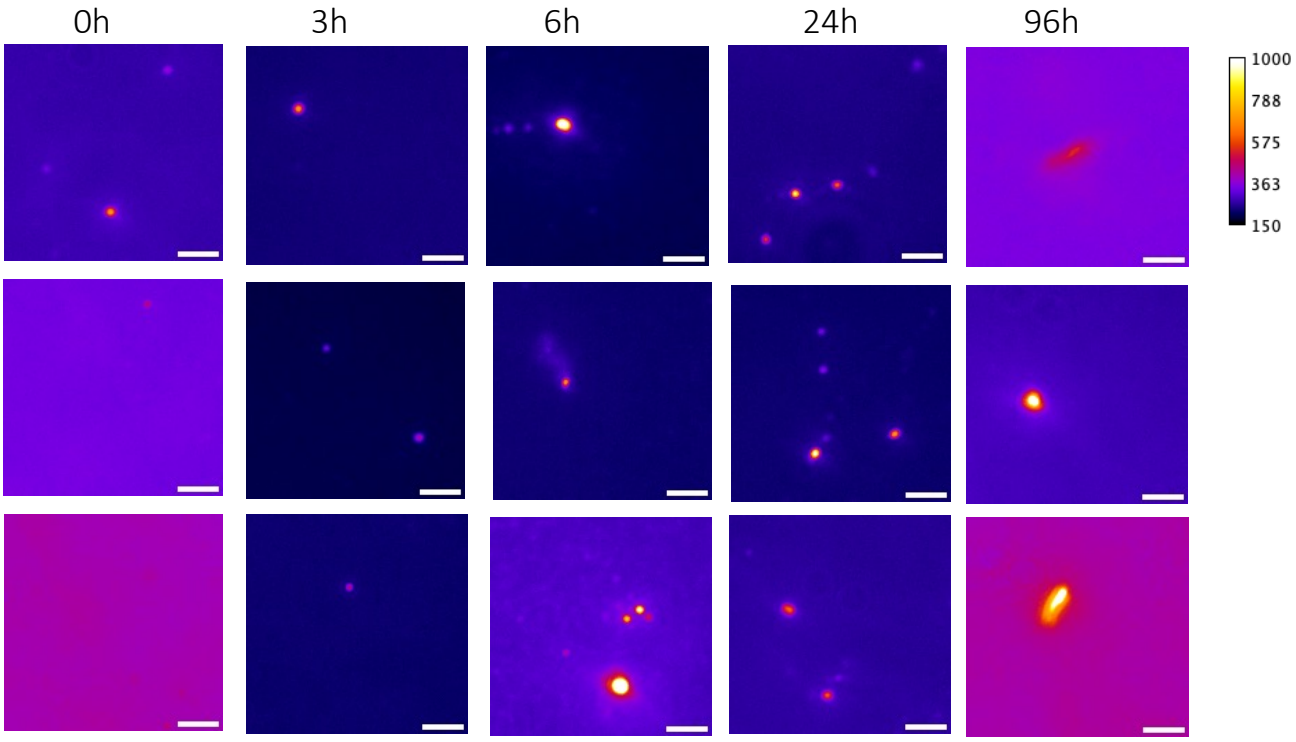

Figure 1: **αSynuclein aggregates extracted at different times during the aggregation process:** Representative images of thioflavin T (ThT) labelled aggregates, obtained using internal reflection microscopy (TIRF), calibration bar indicates fluorescence levels (arbitrary units, AU). Scale bar=2µm. (α-Synuclein: 70µM, kept at 37°C).

The protein species collected at 3h and 96h time points were chosen as representative populations of oligomeric and fibrillar structures, respectively. These populations were further characterized using Nile red (NR) and representative examples are shown in Figure 2. These images were reconstructed using ThunderSTORM (Fiji plugin) to obtain super-resolved images of the aggregates.

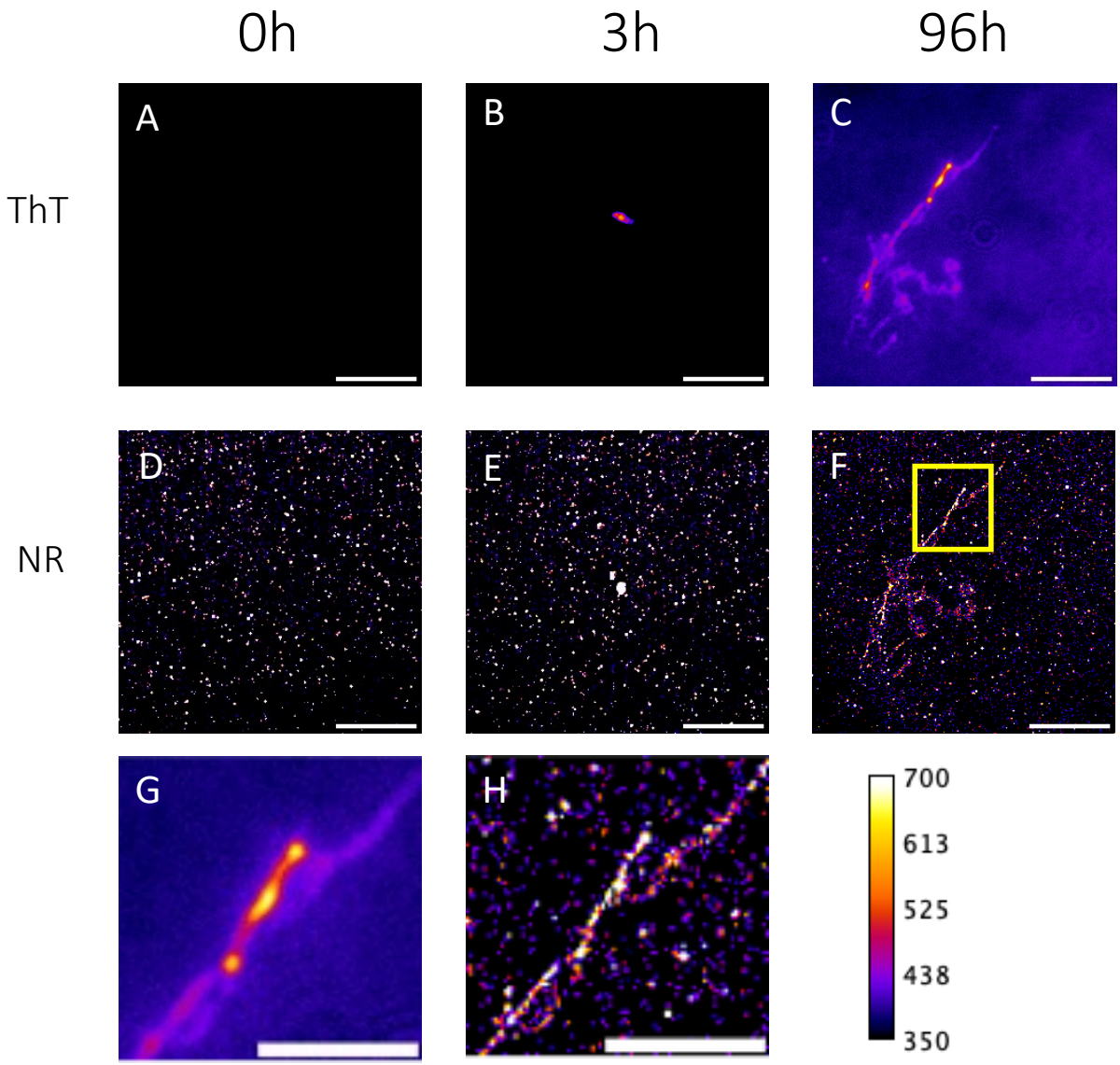

Figure 2: **Comparison of Thioflavin T (ThT) and super resolution Nile Red (NR) imaging for αSynuclein aggregates: A-C** are representative images of αSynuclein aggregates stained with ThT, calibration bar indicates fluorescence levels (arbitrary units, AU). **D-F are** corresponding super-resolved images of NR. Scale bar=5µm. G-H are magnified images of protein fibril C and F with ThT and NR respectively. Scale bar=3µm.

In the given examples, the 96h aggregate (Figure 2C) has a length of more than 10µm. These observations were consistent between the ThT and NR data. Based on their pronounced

differences in structural complexity, 3h and 96h aggregates were selected for the treatment of OHBS.

2. **Detecting astrocytic calcium waves in organotypic hippocampal brain slices (OHBS)**

Figure 3A shows a low magnification image of the hippocampus where the different regions can be observed. Figure 3B shows a high magnification image of an astrocyte expressing GCaMP3. GCaMP3 is a calcium indicator used to detect intracellular calcium fluctuations *in vitro*.

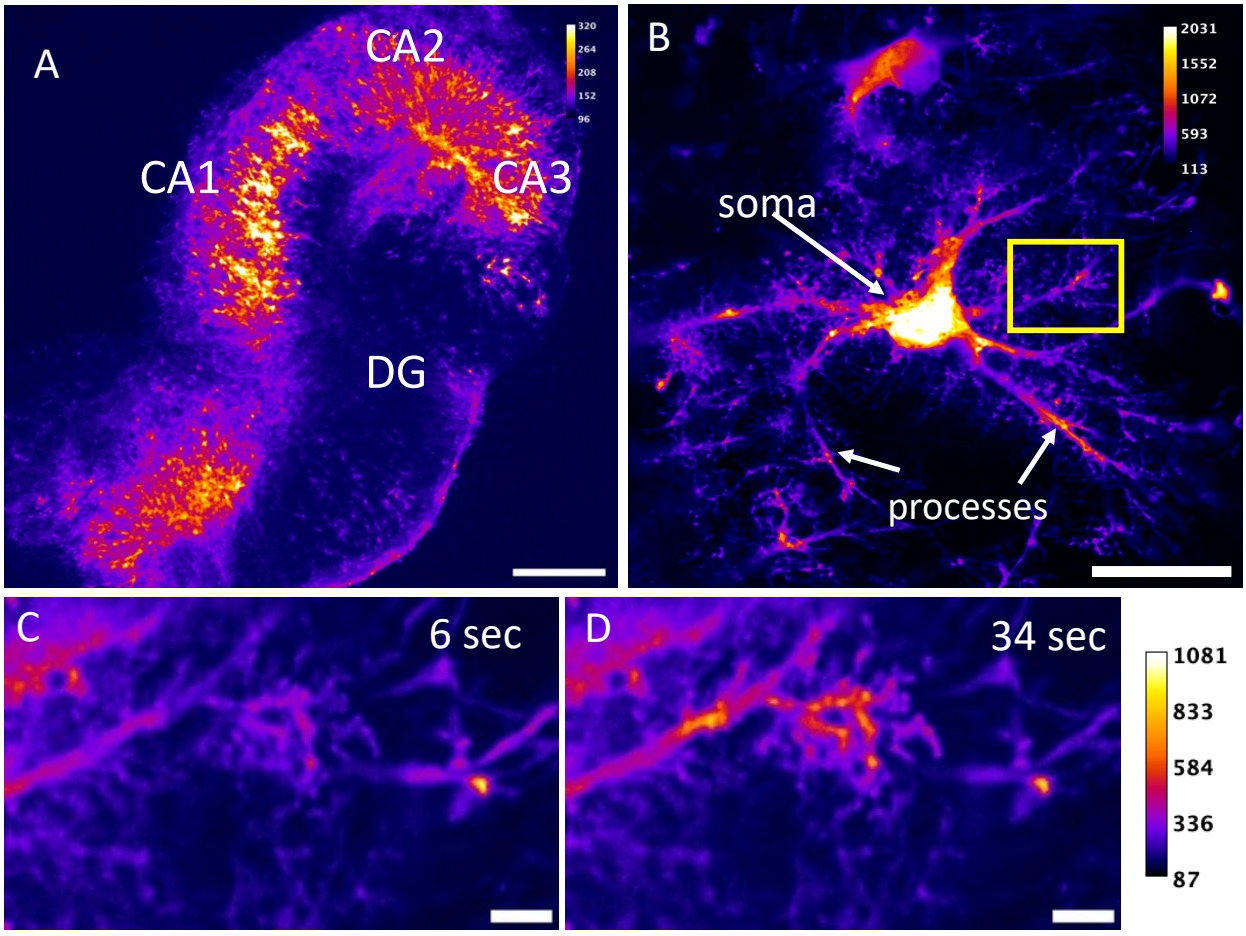

Figure 3: **Murine organotypic hippocampal brain slices (OHBS) as in vitro model to study astrocyte calcium signaling: A** Representative image of an OHBS with indicated dentate gyrus (DG), and the cornu ammonis fields (CA1-CA3). Calcium reporter (GCAMP3) signal is shown in dynamic fire lookup table, calibration bar indicates fluorescence levels (arbitrary units, AU) **B**

Maximum projection of GCAMP3 fluorescence signal in a hippocampal astrocyte with soma and processes indicated with white arrows. Scale bar=500μm. **C** A magnified image of the highlighted area in B, showing an astrocytic process. D The astrocytic process with high calcium signaling. Fluorescence can be seen with the calcium reporter (GCAMP3) signal shown in dynamic fire lookup table, calibration bar indicates fluorescence levels (arbitrary unit) Scale bar=50μm.

An example of astrocytic process is shown in Figure 3C and 3D where a calcium wave propagates through the structure. Supplementary videos 1 and 2 are examples of astrocytic calcium waves. This model allowed us to reliably observe astrocytic calcium waves in OHBSs.

3. Effects of αSynuclein aggregate treatment on astrocytic calcium waves in OHBSs

Oligomeric and fibrillar αSynuclein populations (Figure 2) were used to treat OHBS to observe the effect this would have on astrocytic calcium waves. In order to quantify these effects we characterized astrocytic calcium events by measuring the event frequency, signal area (μm^2), the signal fluorescence (dF/F0), the signal duration (s) and the signal propagation (μm).

a. Event frequency

The event frequency represents the number of detected astrocytic measured in calcium events per minute (epm). Figure 4B shows a visual representation of the events detected in astrocytes treated with 96h αSynuclein compared to the raw data Figure 4A of the same field of view an acquired astrocyte treated with 96h αSynuclein. As seen in Figure 4C there is no statistical difference between the event frequency in both astrocytes treated with 3h αSynuclein and 96h αSynuclein compared to the control. However, there is a marginal increase in median frequency of events between the 3h (1126±667epm) and 96h treatment (2903±1670epm) that is not seen in the control (1895± 724emp).

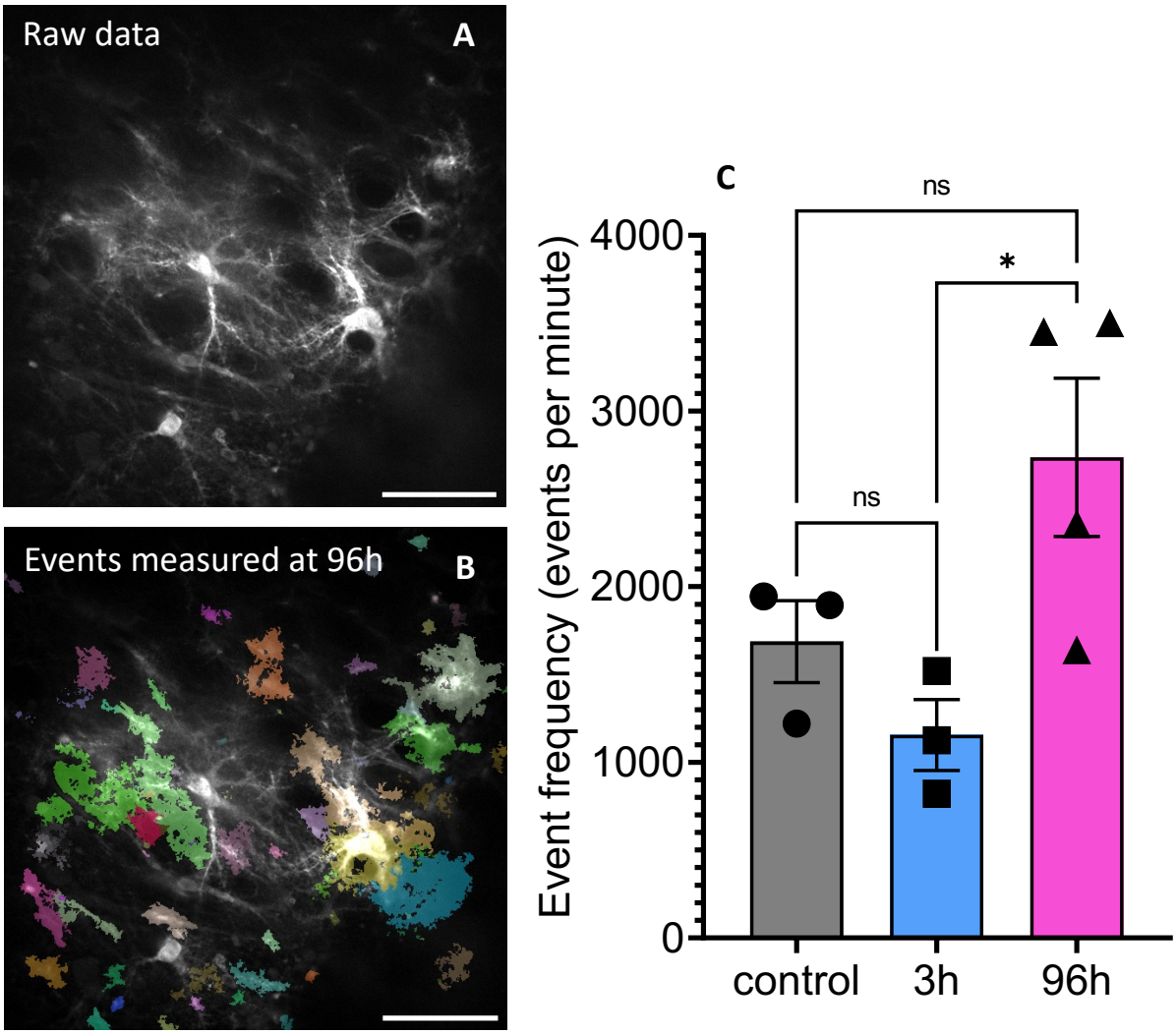

Figure 4: Event frequency of astrocytic calcium waves calcium waves is changed by αSynuclein aggregates in a structure-dependent manner: A. A representative image of the raw data of a field of view with astrocytes treated with 96h αSynuclein. B Example calcium event detection by AQuA in the same field of view. Scale bar=50μm. C Bar plot showing the event frequency (events per minute) where neither 3h nor 96h aggregates affected calcium wave frequency compared to the control $F(2, 7) = 2.874$, $p = 0.1227$. There was a marginal increase in event frequency between 3h and 96h. Analysis was conducted using a Kruskal-Wallis test followed by a Brown-Forsythe post-hoc analysis. 0.1234 (ns), 0.0332 (*), 0.0021 (**), 0.0002 (***), < 0.0001 (****).

b. Signal area

The signal area reflects the size of the calcium waves, showing the maximum area occupied by the wave in μm^2. As seen in Figure 5A, astrocytes treated with 96h αSynuclein had the highest amount of short calcium waves with small areas (Figure 5B) despite having the largest number of events (Figure 4) These results are presented in a violin plot and statistical analysis was carried out (Figure 5C). Calcium waves in astrocytes treated with 96h αSynuclein species had the biggest reduction of wave area ($446.6\mu m^2 \pm 1052.2\mu m^2$). The median signal area had a small reduction for astrocytes treated with 3h αSynuclein ($1029\mu m^2 \pm 2662.2\mu m^2$) compared to the control ($1119\mu m^2 \pm 2808.6\mu m^2$).

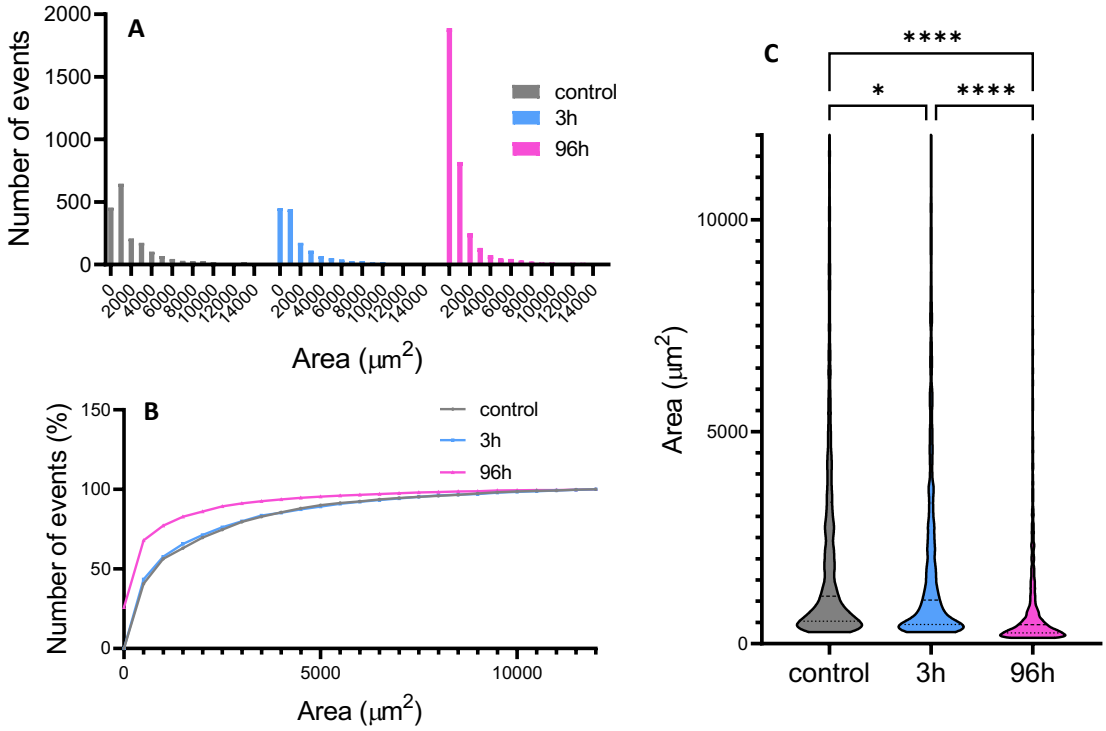

Figure 5: **Area of calcium waves is reduced by αSynuclein aggregates in a structure-dependent manner: A.** Frequency plot showing the number of events and their area (μm^2). **B.** Cumulative frequency plot showing the signal area plotted against the normalized number of events (represented as a percentage) **C.** αSynuclein oligomers (3h) and fibrils (96h) affected calcium wave area (H(2) = 804.3, p <.0001 ****), whereby fibrils caused a stronger reduction. Analysis

was conducted using a Kruskal-Wallis test followed by a Dunn post-hoc analysis. 0.1234 (ns), 0.0332 (*), 0.0021 (**), 0.0002 (***), < 0.0001 (****).

c. Signal fluorescence

The signal fluorescence represents the peak of the dF/F0 curve for each calcium wave. This is the peak difference between the initial fluorescence intensity at resting state and after stimulation (measured in arbitrary units). As seen in Figure 6A, astrocytes treated with 3h αSynuclein have a higher number of events with a lower fluorescence (compared to the control) whereas astrocytes treated with 96h αSynuclein have a lower number of events at a lower fluorescence and events with much higher fluorescence (compared to the control). These results are presented in a violin plot and statistical analysis was carried out (Figure 6C). Calcium waves in astrocytes treated with αSynuclein 96h had an increase in fluorescence (0.5091au ± 0.3536au) compared to the control. Lastly, astrocytes treated with 3h αSynuclein have a lower median signal fluorescence (0.3453au ± 0.1941au) compared to the control (0.3986au ± 0.2593au).

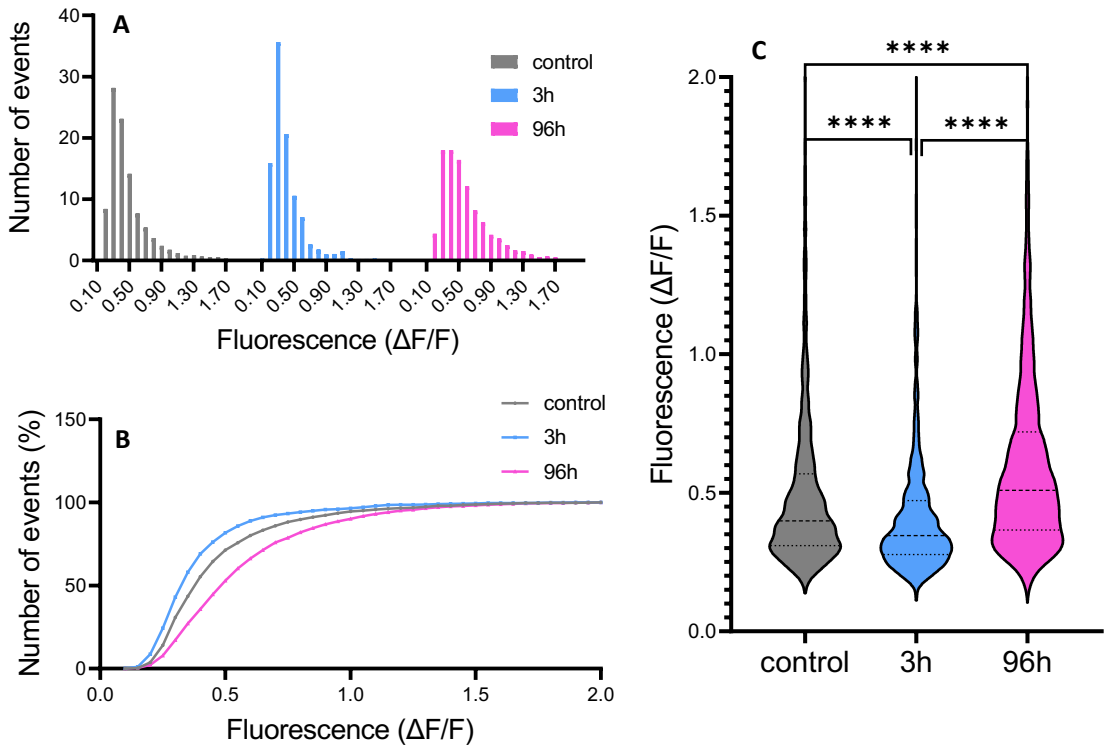

Figure 6**: Fluorescence of calcium waves is changed by αSynuclein aggregates in a structure-dependent manner: A.** Frequency plot showing the number of events and their fluorescence (ΔF/F). **B.** Cumulative frequency plot showing the signal fluorescence plotted against the normalized number of events (represented as a percentage) **C.** αSynuclein oligomers (3h) and fibrils (96h) affected calcium wave area (H(2) = 618.7, p <.0001 ****), whereby oligomers caused a reduction and fibrils caused an increase. Analysis was conducted using a Kruskal-Wallis test followed by a Dunn post-hoc analysis. 0.1234 (ns), 0.0332 (*), 0.0021 (**), 0.0002 (***), < 0.0001 (****).

d. Signal duration

The signal duration records the time at 50% onset point of an event to 50% offset time point of the same event in seconds. As seen in Figure 7A, astrocytes treated with 3h αSynuclein have less events with a higher duration as compared to astrocytes treated with 96h αSynuclein (Figure 7C). Calcium waves in astrocytes treated with 96h αSynuclein have a longer median duration(6.00s ± 4.85s) compared to the control (1.95s ± 1.6s). Whereas astrocytes treated with 3h αSynuclein

have a marginal decrease of median duration of calcium waves (1.70s ± 1.7s) compared to the control.

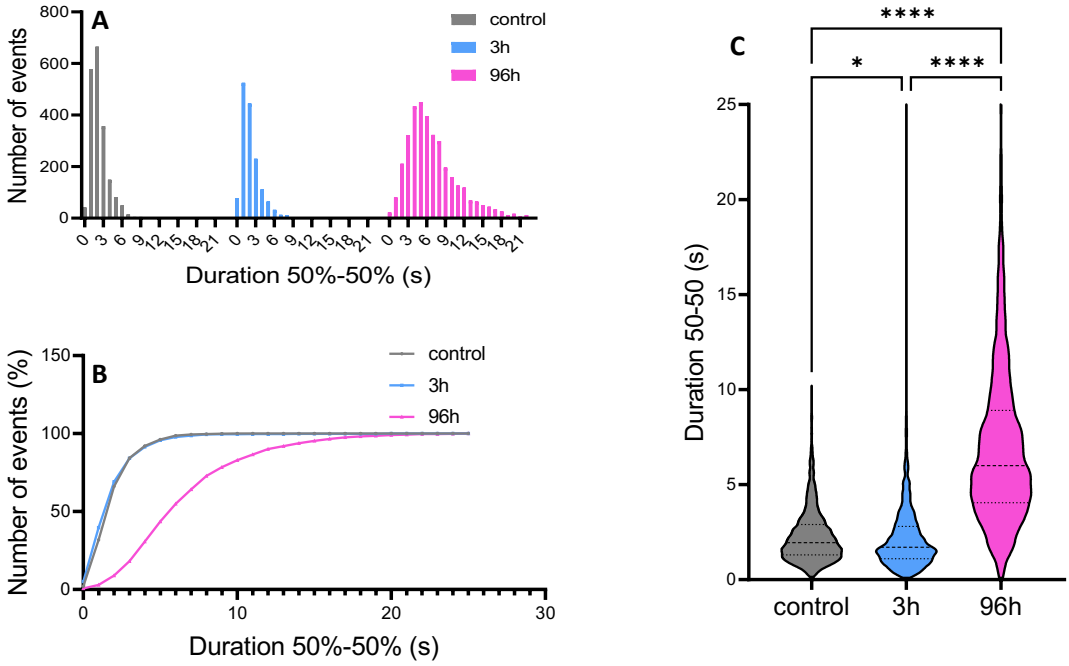

Figure 7: **Duration of calcium waves is changed by αSynuclein aggregates in a structure-dependent manner: A.** Frequency plot showing the number of events and their duration (s). **B.** Cumulative frequency plot showing the signal duration plotted against the normalized number of events (represented as a percentage) **C.** αSynuclein oligomers (3h) and fibrils (96h) affected calcium wave area (H(2) = 3351, p <.0001 ****), whereby oligomers caused a marginal decrease in duration and fibrils caused an increase. Analysis was conducted using a Kruskal-Wallis test followed by a Dunn post-hoc analysis. 0.1234 (ns), 0.0332 (*), 0.0021 (**), 0.0002 (***), < 0.0001 (****).

e. Signal propagation

The signal propagation is a measure of a single event through the sum of distances of all frames from where the calcium signal started (μm). As seen in Figure 8A, both astrocytes treated with 3h αSynuclein and 96h αSynuclein have a high number of events with a lower propagation distance

compared to control astrocytes. As seen in both Figure 8B and Figure 8C there is no difference in the astrocytic calcium waves between 3h αSynuclein and 96h αSynuclein (Figure 8C). Calcium waves in astrocytes treated with αSynuclein 96h (2.596 μm ± 11.301μm) and 3h (3.361μm ± 16.94μm) have a lower onset propagation compared to the control (4.713μm ± 19.301μm).

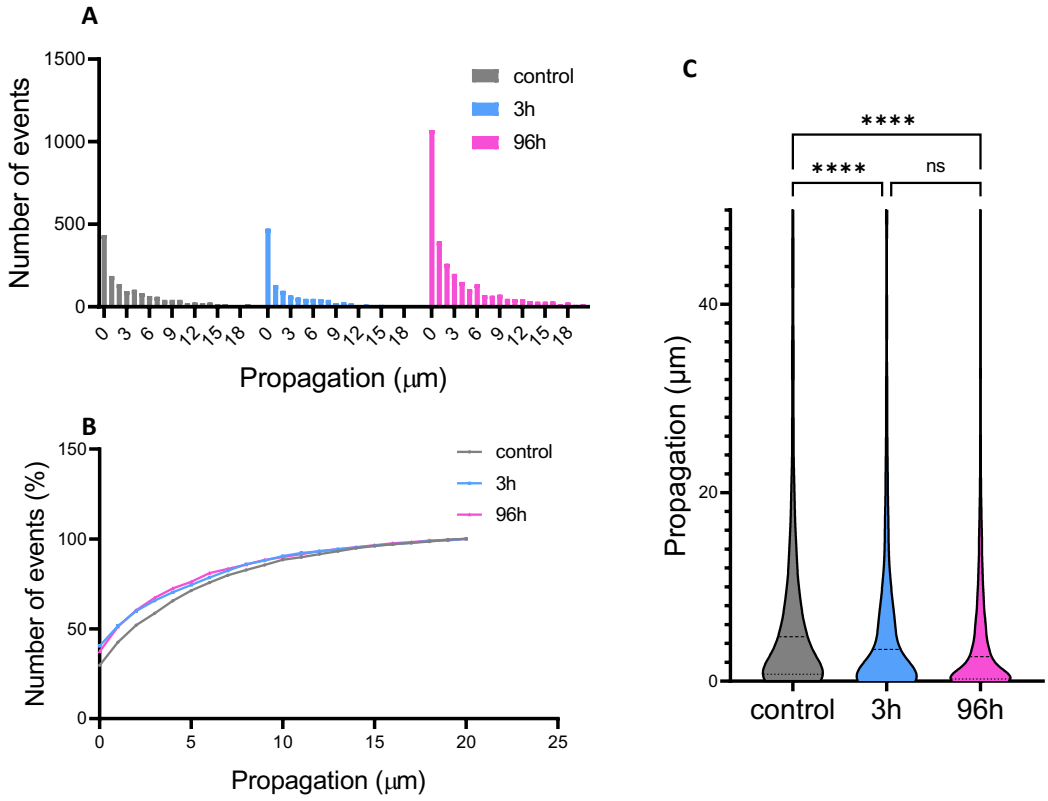

Figure 8: **Propagation of calcium waves is decreased by αSynuclein aggregates in a structure-dependent manner: A.** Frequency plot showing the number of events and their propagation (mm). **B.** Cumulative frequency plot showing the signal propagation plotted against the normalized number of events (represented as a percentage) **C.** αSynuclein oligomers (3h) and fibrils (96h) affected calcium wave area (H(2) = 56.83, p <.0001 ****), whereby there is no significant difference between oligomers and fibrils. Analysis was conducted using a Kruskal-Wallis test followed by a Dunn post-hoc analysis. 0.1234 (ns), 0.0332 (*), 0.0021 (**), 0.0002 (***), < 0.0001 (****).

Discussion:

In this study, we investigated the effect that different αSynuclein aggregates had on calcium waves in astrocytes from OHBSs. This was done through the characterization of αSynuclein aggregates, using super resolution imaging and live imaging of astrocytic calcium waves in hippocampal slices. It was found that αSynuclein affects astrocytic calcium waves in a structure dependent way.

Numerous studies have reported that fibril and oligomer αSynuclein aggregates have different effects on nerve cells. Oligomeric αSynuclein species are reported as toxic whereas fibrils are pro-inflammatory and protective.[18,19,20,21,22]

Astrocytes respond to neuron-derived αSynuclein by releasing proinflammatory factors, triggering microglial activation. Small αSynuclein amounts cause prolonged inflammation, damaging neurons αSynuclein from damaged neurons triggers astrocytic dysfunction, inflammation, and impaired protein degradation.[40,41]

This study showed that αSynuclein fibrils had a more prominent effect on astrocytic calcium signaling than. Fibrils caused an increase in calcium wave frequency in comparison with control and oligomer-treated slices (figure 4C) with lowest calcium signal area (figure 5C). However, fibrils-treated slices had the highest calcium signal fluorescence (figure 6C) and duration (figure 7C) whilst maintaining the lowest propagation compared to the control (figure 8C). The opposite was found for αSynuclein oligomers whereby astrocytic calcium waves had the lowest event frequency compared to the control (figure 4C) with a marginal decrease in calcium signal area compared to the control (figure 5C) as well as a lower calcium signal fluorescence (figure 6C) compared to the control and a lower signal duration (figure 7C).

Astrocytes play a crucial role in clearing neurotransmitters, including glutamate through EAAT2.[42] Studies indicate that the internalization of EAAT2 from astrocyte surfaces is regulated by calcium

ion levels.[43] Abnormal dopamine-induced calcium ion signals in astrocytes result in EAAT2 downregulation, leading to elevated extracellular glutamate and neurodegeneration.[44]

The results presented in this study suggest that as fibrils and oligomers could trigger different toxic mechanisms in PD.

If astrocytes treated with fibrillar aggregates have localized and small astrocytic calcium waves, it may lead to EAAT2 downregulation. Moreover, the underpinning mechanisms for the findings in this study could be leading to astrocytic failure that could increases neuronal death due to neuroinflammation. An alternative interpretation of the data is that fibrils may be trigger protective mechanisms in astrocytes.

The results presented in this study emphasize the significance of the astrocytic role in PD. Although the exact sub-cellular mechanisms are still unknown, future work can focus on their depiction and understanding of the implications on neuronal function. This could all give way to a more comprehensive and specialized therapeutic target for PD.

Acknowledgements:

I would like to express my deepest gratitude to Lord Laidlaw and the Laidlaw Foundation as well as Laidlaw team at the University of St Andrews. I would also like to thank Dr Vanya Metodieva and Dr Juan Varela for their ongoing and unwavering support throughout this project and beyond. Lastly, I would like to thank Gema, Carlos, and Samuel immensely for their never-ending support in my research.

References:

[1] Parkinson, J. (2002). An essay on the shaking palsy. *The Journal of neuropsychiatry and clinical neurosciences*, *14*(2), 223-236.

[2] Venda, L. L., Cragg, S. J., Buchman, V. L., & Wade-Martins, R. (2010). α-Synuclein and dopamine at the crossroads of Parkinson's disease. *Trends in neurosciences*, *33*(12), 559-568.

[3] Spillantini, M. G., Schmidt, M. L., Lee, V. M. Y., Trojanowski, J. Q., Jakes, R., & Goedert, M. (1997). A-Synuclein in Lewy bodies. *Nature*, *388*(6645), 839-840.

[4] Goedert, M. (2001). Alpha-synuclein and neurodegenerative diseases. *Nature reviews neuroscience*, *2*(7), 492-501.

[5] Lavedan, C., Buchholtz, S., Auburger, G., Albin, R. L., Athanassiadou, A., Blancato, J., … & Polymeropoulos, M. H. (1998). Absence of Mutation in the β-and γ-Synuclein Genes in Familial Autosomal Dominant Parkinson's Disease. *DNA research*, *5*(6), 401-402.

[6] Mouradian, M. M. (2002). Recent advances in the genetics and pathogenesis of Parkinson disease. *Neurology*, *58*(2), 179-185.

[7] Okuzumi, A., Hatano, T., Matsumoto, G., Nojiri, S., Ueno, S. I., Imamichi-Tatano, Y., … & Hattori, N. (2023). Propagative α-synuclein seeds as serum biomarkers for synucleinopathies. *Nature Medicine*, 1-8.

[8] Calabresi, P., Mechelli, A., Natale, G., Volpicelli-Daley, L., Di Lazzaro, G., & Ghiglieri, V. (2023). Alpha-synuclein in Parkinson's disease and other synucleinopathies: from overt neurodegeneration back to early synaptic dysfunction. *Cell death & disease*, *14*(3), 176.

[9] Braak, H., Ghebremedhin, E., Rüb, U., Bratzke, H., & Del Tredici, K. (2004). Stages in the development of Parkinson's disease-related pathology. *Cell and tissue research*, *318*, 121-134.

[10] Ghosh, D., Singh, P. K., Sahay, S., Jha, N. N., Jacob, R. S., Sen, S. & Maji, S. K. (2015). Structure based aggregation studies reveal the presence of helix-rich intermediate during α-Synuclein aggregation. *Scientific reports*, *5*(1), 9228.

[11] Serpell, L. C. (2000). Alzheimer's amyloid fibrils: structure and assembly. *Biochimica et Biophysica Acta (BBA)-Molecular Basis of Disease*, *1502*(1), 16-30.

[12] Biere, A. L., Wood, S. J., Wypych, J., Steavenson, S., Jiang, Y., Anafi, D., … & Citron, M. (2000). Parkinson's disease-associated α-synuclein is more fibrillogenic than β-and γ-synuclein and cannot cross-seed its homologs. *Journal of Biological Chemistry*, *275*(44), 34574-34579.

[13] Maries, E., Dass, B., Collier, T. J., Kordower, J. H., & Steece-Collier, K. (2003). The role of α-synuclein in Parkinson's disease: insights from animal models. *Nature Reviews Neuroscience*, *4*(9), 727-738.

[14] Cremades, N., Cohen, S. I., Deas, E., Abramov, A. Y., Chen, A. Y., Orte, A., … & Klenerman, D. (2012). Direct observation of the interconversion of normal and toxic forms of α-synuclein. *Cell*, *149*(5), 1048-1059

[15] Brown, D. R. (2010). Oligomeric alpha-synuclein and its role in neuronal death. *IUBMB life*, *62*(5), 334-339.

[16] Karpinar, D. P., Balija, M. B. G., Kügler, S., Opazo, F., Rezaei-Ghaleh, N., Wender, N. & Zweckstetter, M. (2009). Pre-fibrillar α-synuclein variants with impaired β-structure increase neurotoxicity in Parkinson's disease models. *The EMBO journal*, *28*(20), 3256-3268.

[17] Wright, J. A., Wang, X., & Brown, D. R. (2009). Unique copper-induced oligomers mediate alpha-synuclein toxicity. *The FASEB Journal*, *23*(8), 2384-2393

[18] Emin, D., Zhang, Y. P., Lobanova, E., Miller, A., Li, X., Xia, Z., … & Klenerman, D. (2022). Small soluble α-synuclein aggregates are the toxic species in Parkinson's disease. *Nature communications*, *13*(1), 5512.

[19] Caughey, B., & Lansbury Jr, P. T. (2003). Protofibrils, pores, fibrils, and neurodegeneration: separating the responsible protein aggregates from the innocent bystanders. *Annual review of neuroscience*, *26*(1), 267-298.

[20] Brück, D., Wenning, G. K., Stefanova, N., & Fellner, L. (2016). Glia and alpha-synuclein in neurodegeneration: A complex interaction. *Neurobiology of disease*, *85*, 262-274.

[21] Cornell-Bell, A. H., & Finkbeiner, S. M. (1991). Ca2+ waves in astrocytes. *Cell calcium*, *12*(2-3), 185-204.

[22] Bundgaard, M., & Abbott, N. J. (2008). All vertebrates started out with a glial blood-brain barrier 4–500 million years ago. *Glia*, *56*(7), 699-708.

[23] Lee, H. W., Xu, Y., Zhu, X., Jang, C., Choi, W., Bae, H., … & Simons, M. (2022). Endothelium-derived lactate is required for pericyte function and blood–brain barrier maintenance. *The EMBO journal*, *41*(9), e109890.

[24] Vainchtein, I. D., Chin, G., Cho, F. S., Kelley, K. W., Miller, J. G., Chien, E. C., … & Molofsky, A. V. (2018). Astrocyte-derived interleukin-33 promotes microglial synapse engulfment and neural circuit development. *Science*, *359*(6381), 1269-1273.

[25] Pekny, M., Pekna, M., Messing, A., Steinhäuser, C., Lee, J. M., Parpura, V., … & Verkhratsky, A. (2016). Astrocytes: a central element in neurological diseases. *Acta neuropathologica*, *131*, 323-345.

[26] Haim, L. B., & Escartin, C. (2022). Astrocytes and neuropsychiatric symptoms in neurodegenerative diseases: Exploring the missing links. *Current Opinion in Neurobiology*, *72*, 63-71.

[27] Kettenmann, H., Backus, K. H., & Schachner, M. (1987). Γ-Aminobutyric acid opens Cl-channels in cultured astrocytes. *Brain research*, *404*(1-2), 1-9.

[28] Orkand, R. K. (1986). Introductory remarks: Glial-interstitial fluid exchange. *Annals of the New York Academy of Sciences*, *481*(1), 269-272.

[29] Prince, D. A. (1978). Neurophysiology of epilepsy. *Annual review of neuroscience*, *1*(1), 395-415.

[30] Kim, Y. S., & Joh, T. H. (2006). Microglia, major player in the brain inflammation: their roles in the pathogenesis of Parkinson's disease. *Experimental & molecular medicine*, *38*(4), 333-347.

[31] Dong, Z., Saikumar, P., Weinberg, J. M., & Venkatachalam, M. A. (2006). Calcium in cell injury and death. *Annu. Rev. Pathol. Mech. Dis.*, *1*, 405-434.

[32] Semyanov, A., Henneberger, C., & Agarwal, A. (2020). Making sense of astrocytic calcium signals—from acquisition to interpretation. *Nature Reviews Neuroscience*, *21*(10), 551-564.

[33] Bazargani, N., & Attwell, D. (2016). Astrocyte calcium signaling: the third wave. *Nature neuroscience*, *19*(2), 182-189.

[34] Finkbeiner, S. (1992). Calcium waves in astrocytes-filling in the gaps. *Neuron*, *8*(6), 1101-1108.

[35] Shigetomi, E., Saito, K., Sano, F., & Koizumi, S. (2019). Aberrant calcium signals in reactive astrocytes: a key process in neurological disorders. *International journal of molecular sciences*, *20*(4), 996.

[36] Ding, S. (2013). In vivo astrocytic Ca2+ signaling in health and brain disorders. *Future neurology*, *8*(5), 529-554.

[37] Nimmerjahn, A. (2009). Astrocytes going live: advances and challenges. *The Journal of physiology*, *587*(8), 1639-1647.

[38] Filosa, J. A., Bonev, A. D., Straub, S. V., Meredith, A. L., Wilkerson, M. K., Aldrich, R. W., & Nelson, M. T. (2006). Local potassium signaling couples neuronal activity to vasodilation in the brain. *Nature neuroscience*, *9*(11), 1397-1403.

[39] Wang, Yizhi, et al. Accurate quantification of astrocyte and neurotransmitter fluorescence dynamics for single-cell and population-level physiology. *Nature neuroscience*, 2019, vol. 22, no 11, p. 1936-1944.

[40] Lee, H. J., Kim, C., & Lee, S. J. (2010). Alpha-synuclein stimulation of astrocytes: Potential role for neuroinflammation and neuroprotection. *Oxidative medicine and cellular longevity*, *3*, 283-287.

[41] Wang, C., Yang, T., Liang, M., Xie, J., & Song, N. (2021). Astrocyte dysfunction in Parkinson's disease: from the perspectives of transmitted α-synuclein and genetic modulation. *Translational Neurodegeneration*, *10*, 1-17.

[42] Bancroft, E. A., & Srinivasan, R. (2022). Emerging Roles for Aberrant Astrocytic Calcium Signals in Parkinson's Disease. *Frontiers in Physiology*, *12*, 812212.

[43] Ambrosi, G., Cerri, S., & Blandini, F. (2014). A further update on the role of excitotoxicity in the pathogenesis of Parkinson's disease. *Journal of neural transmission*, *121*, 849-859.

[44] Xin, W., Schuebel, K. E., Jair, K. W., Cimbro, R., De Biase, L. M., Goldman, D., & Bonci, A. (2019). Ventral midbrain astrocytes display unique physiological features and sensitivity to dopamine D2 receptor signaling. *Neuropsychopharmacology*, *44*(2), 344-355.

Supplementary data:

Video one: OHBS astrocytic calcium wave signaling.

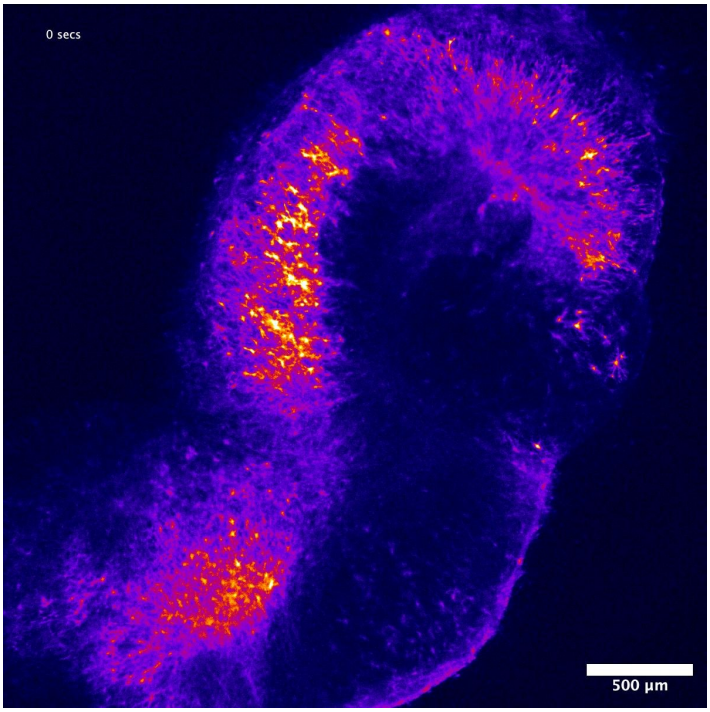

Video two: Astrocytic Calcium signaling.

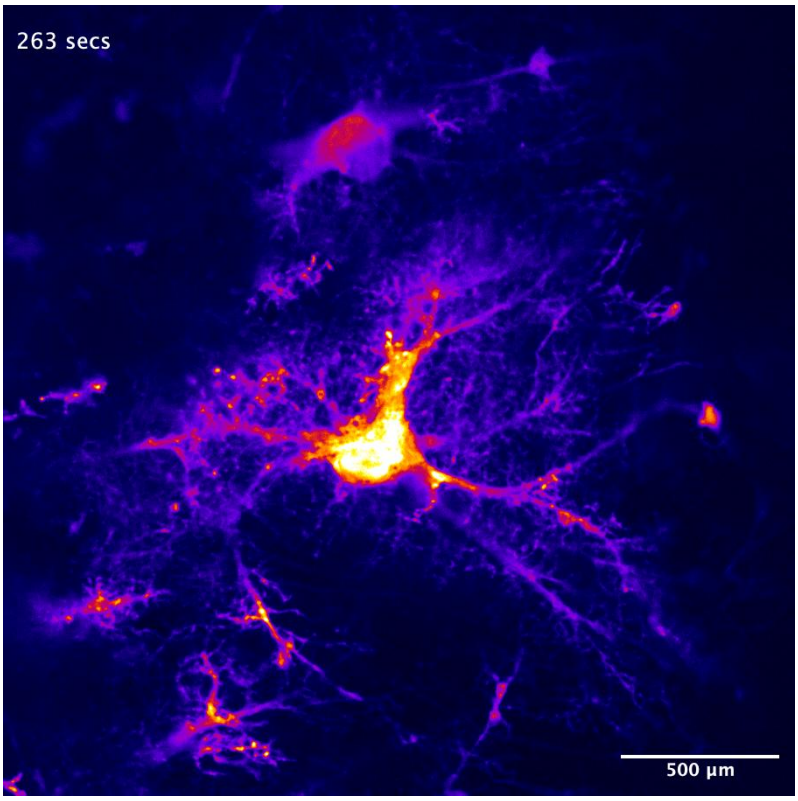

Video three: Astrocytic calcium wave events.

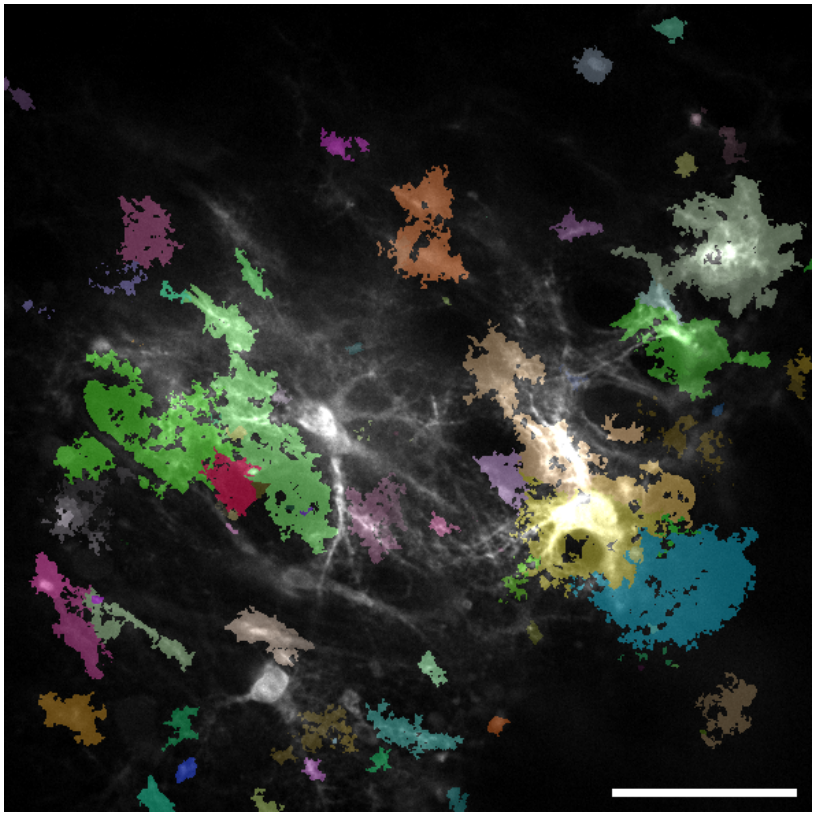

Video four: Z-stack representation of an astrocyte.